Self-Assembled Monolayer as a Template to Deposit Silicon Nanoparticles Fabricated by Laser Ablation

K. Hata,*,†,‡ S. Yoshida, M. Fujita, S. Yasuda, T. Makimura, K. Murakami, and H. Shigekawa§

Institute of Applied Physics and CREST, Japan Science and Technology Corporation (JST), University of Tsukuba, Tennodai 1-1-1, Tsukuba 305-8573, Japan

Received: February 28, 2001; In Final Form: June 17, 2001

We demonstrate a use of self-assembled monolayer (SAM) as a template to deposit in-situ Si nanoparticles fabricated by laser ablation. Scanning tunneling microscopy, atomic force microscopy observations, and photoluminescence measurements show that the Si nanoparticles deposited in situ on SAMs are round shaped, firmly attached to the surface, and remain stable for at least a couple of months. Control over the average size of the Si nanoparticles could be achieved, in the region where quantum confinement effect is important, by changing the Ar ambient pressure. Our results show that SAM endures the fierce heat, ions, and plasma generated during the laser ablation process, and the use of SAM could be extended as a substrate to deposit in-situ materials fabricated by laser ablation. In-situ deposition is important because it would facilitate fabrication of high functional nanoarchitectures based on this easily oxidized material. We believe that the wide range of available SAMs, different in chemical and electronic functionality, combined with the wide variety of nanostructures possible to fabricate by laser ablation, would open up a new opportunity to assemble these nanomaterials into high functional complexities of the next level.

1. Introduction

The self-assembled monolayer (SAM) stands as a unique and promising building block to fabricate rational nanodevices. One route to fabricate highly functional nanoarchitectures by SAM is to use SAM as a template to deposit and immobilize functional nanostructures or molecules rather than exploring the use of SAM itself. Even though this direction has not been explored so intensely so far, the ease of control of the chemical functionality of the surface of SAM and the ability to pattern SAM by the microcontact printing method[1] might prove important in the future. Some examples of nanostructures immobilized and templated on SAM include: Au nanoparticles,[2,3] carbon nanotubes,[4] polymers,[5] and organic molecules.[6] Here we introduce a new entry to this list, Si nanoparticles.

Nanoparticles readily exhibit quantum phenomena and are hopefully the ideal candidate as building blocks for the next generation devices.[7] Silicon nanoparticle is a promising candidate because (1) it shows visible photoluminescence[8] that is related to a quantum confinement effect, (2) the wavelength of photoluminescence is tunable,[9] and (3) the reason an indirect band gap material as Si shows photoluminescence with high quantum efficiency when formed into a nanostructure is not clearly understood, a fact that poses a challenge to basic physics and chemistry.[10] The most simple and prevailed method to fabricate Si nanoparticles is to etch Si wafers in a solution of hydrofluoric acid, a procedure that produces porous Si.[8] Basically, colloidal Si nanoparticles can be produced from this porous Si and transferred to another template,[11] though the size and surface states of these particles are highly heterogeneous. This aspect is critically undesirable because these two factors mainly determine the optical and electronic properties of a particle.[10]

Laser ablation is an alternative method that has the ability to fabricate pure, well characterized, and relatively uniform Si nanoparticles.[12−15] The laser ablation method possesses its own unique strengths, including (1) control over the size of the nanoparticle,[13,14] (2) wide variety of nanostructures possible to fabricate, including, fluerene,[16] carbon nanotubes,[17] nanowires,[18] and Si nanoparticles,[12−15] and (3) the ability to fabricate nanostructures with impurities embedded.[19,20] The last point might become important in future aspects of nanoparticle engineering and is difficult to achieve by colloidal synthesis.

On the other hand, heat, plasma, and ions generated during the laser ablation process are harmful and might prevent the use of soft organic materials as a deposition substrate. Actually, in the past, most of the previous studies have used robust materials such as oxidized Si layers for a deposition substrate. Here we demonstrate that it is possible to deposit in situ Si nanoparticles fabricated by laser ablation on SAM substrates. Our results demonstrate that the use of SAM as a template could be extended even into the very fierce environment of laser ablation. Achievement of in situ deposition would be very important in future applications since sequential processes could be carried out in a vacuum after deposition without exposing these easily oxidized material to air. We believe that the wide range of available SAMs, different in chemical and electronic functionality, combined with the wide variety of nanostructures possible to fabricate by laser ablation would open up a new opportunity to assemble these nanomaterials into new nanoarchitectures.

2. Experimental Section

2.1. Materials. Epitaxial Au(111) surfaces (50 nm thick) were prepared by resistive evaporation at a rate of 0.06 nm/s onto

* Author to whom correspondence should be addressed.
† E-mail: khata@cmliris.harvard.edu.
‡ Present address: Department of Chemistry and Chemical Biology, Harvard University, Cambridge, MA 02138.
§ E-mail: hidemi@ims.tsukuba.ac.jp, http://dora.ims.tsukuba.ac.jp.

10.1021/jp010760b CCC: $20.00
Published on Web 10/12/2001

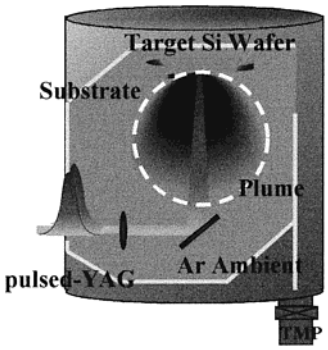

Figure 1. A schematic of the laser ablation chamber.

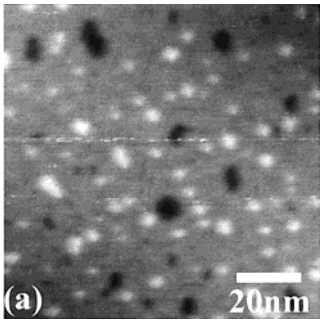

Figure 2. A typical STM image of the SAM (hexanethiol) substrate exposed to ablation. This image was taken approximately 1 cm from the ablation spot. White protrusions observed are Si nanoparticles deposited on SAM. Ablation conditions: Ar ambient pressure 5 Torr, 100 shots. Tunneling conditions: surface bias = 500 mV, tunneling current = 500 pA. No eminent dependence on tunneling conditions was observed.

freshly cleaved mica heated to 500 °C. The vacuum pressure during the evaporation was 6×10^{-6} Torr. Before use, Au(111) surfaces were cleaned by hydrogen flame annealing. A terrace and stepped surface with grain sizes of 100−200 nm was observed by scanning tunneling microscope (STM) and the existence of the herringbone structure was confirmed in some high-resolution images. SAM was prepared on these Au(111) substrates by adsorption of hexanethiol (Wako, used as received) from millimolar solutions in ethanol at room temperature for 12 to 24 h. All monolayes were rinsed with ethanol after adsorption and dried under a flow of N_2. All the resulting samples were characterized using a scanning probe microscope (Nanoscope III system, Digital Instruments), and a tapping mode noncontact atomic force microscope (AFM) (SPA 300HV system (Seiko)).

2.2. Laser Ablation. A schematic of the ablation chamber is shown in Figure 1. A part of a Si wafer was placed close to the focal point of the laser beam. The SAM substrate was placed on the same plane of the target wafer and the typical distance from the ablation spot was approximately 5 mm. The chamber was evacuated to 5×10^{-7} Torr, and then filled with Ar gas (purity 99.9999%), with a pressure ranging from 2 to 10 Torr. A predetermined number of YAG pulsed laser shots (10 ns, 5 J/cm^2) were focused and irradiated to the target Si wafer at frequencies of 1 or 10 Hz. Si nanoparticles formed by collision of the hot Si atoms in the plasma with the inert gas are supposed to land softly on the SAM.

3. Results and Discussion

Figure 2 shows a typical STM image of the surface of SAM exposed to laser ablation. Before ablation, the surface is covered with numerous etch-pits. Their density and size are similar to

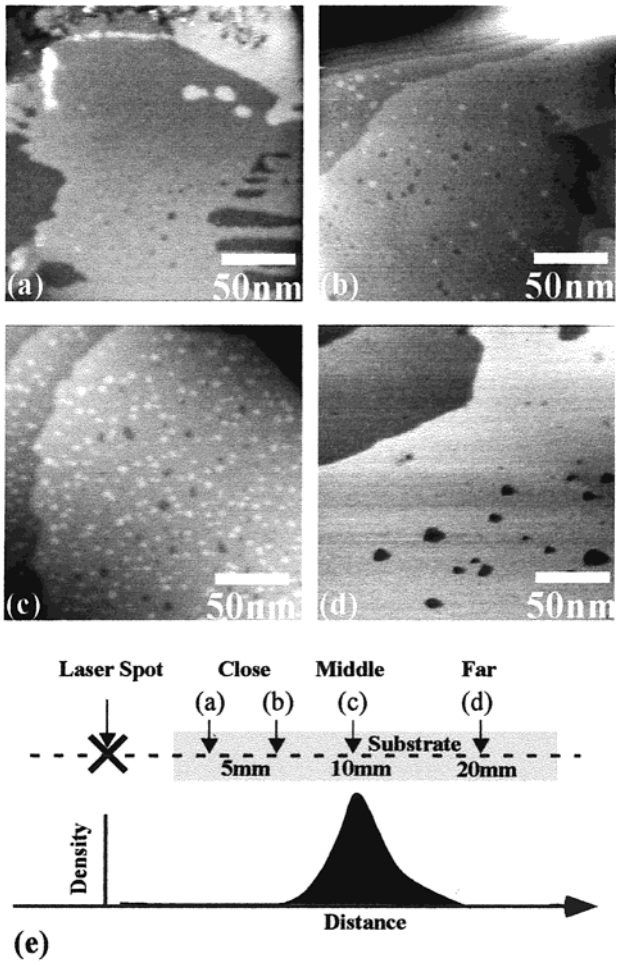

Figure 3. A set of STM images of the same SAM (hexanethiol) substrate exposed to ablation taken at different distances from the ablation shot. Ablation conditions: Ar ambient pressure 5 Torr, 100 shots. (e) Schematic showing the distance of each image from the ablation spot. Histogram schematically shows the density of the Si nanoparticles versus distance from the ablation spot.

previous reports,[21] which we consider as an evidence of a successful formation of SAM. After ablation, many bright protrusions are observed that have a size of 5 to 10 nm when the Ar ambient is 5 Torr. On the other hand, the heights of the protrusions in the STM images were around 0.4 nm, a value substantially smaller than their lateral size,[22] a point that would be discussed later. The density of the protrusions depends strongly on the distance from the ablation spot. This aspect is demonstrated by a set of STM images in Figure 3 taken on the same sample at different distances from the ablation spot. Very close to the ablation spot (Figure 3a) only a very small number of protrusions were observed, and also the density of the etch-pits had significantly decreased (close region). At a distance of 6 mm from the ablation spot (Figure 3b), a small number of protrusions were observed which density increases with distance. The density of the protrusions maximize at a distance approximately 1 cm from the ablation spot (Figure 3c), and then decreases with distance (middle region). At 2 cm from the ablation spot (Figure 3d) no protrusions were observed, and a surface was clean SAM (far region). When the fact that almost no SAM and protrusions were observed very close to the ablation spot and the fierce circumstance during the ablation process (heat, ions, and plasma) are considered, it is possible that SAM, particularly those close to the ablation spot, is demolished or rearranged and observed as protrusions in the

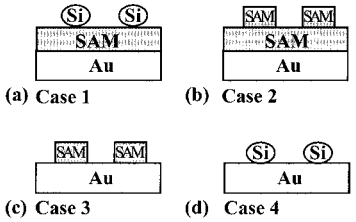

Figure 4. (a) Case 1: white protrusions are Si nanoparticles deposited on SAM. (b) Case 2: protrusions are SAM islands on SAM. (c) Case 3: Protrusions are SAM islands on Au. (d) Case 4: Protrusions are Si nanoparticles on Au.

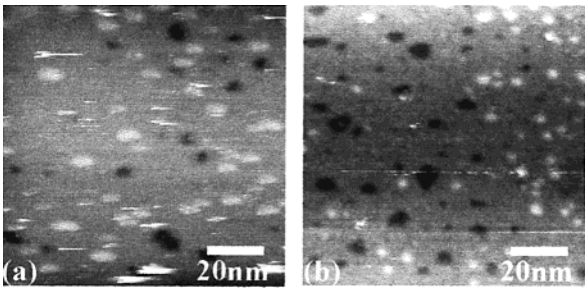

Figure 5. (a) An STM image of a SAM (hexanethiol) substrate exposed to ablation before ethanol rinse. (b) An STM image of the same sample after ethanol rinse.

STM images. Figure 4 shows schematics of the possible cases that must be considered. Case 1: SAM endures the ablation process and the protrusion observed are indeed Si nanoparticles deposited on SAM (Si nanoparticles on SAM). Case 2: Protrusions observed are fragments of SAM blown away from some part of the SAM (probably closer to the ablation spot) during the ablation process (SAM islands on SAM − no particles). Case 3: SAM is partly blown way (SAM island on Au − no particles). Case 4: SAM is completely blown away and the protrusions are Si nanoparticles deposited on Au (particles on Au). Several tests based on known characteristics of SAM were carried out to eliminate case 2 to 4, and to verify the successful deposition of Si nanoparticles on SAM.

3.1. Case 2: SAM Islands on SAM. It is possible that SAM close to the ablation spot is blown away during the laser ablation process and redeposit onto undamaged SAM farther from the ablation spot. From this standpoint, the observed dependence of the density of the protrusions in the STM images with distance from the ablation spot is readily explained. No SAM was observed very close to the ablation spot because they were blown away. They redeposit at locations farther and rearrange and are observed as protrusions in the STM images. Regions far away remains untouched, hence a clean SAM is observed there. We eliminate this possibility by considering the physical properties of bilayer SAM. SAM only weakly physisorbs on SAM and is easily washed away by rinsing in ethanol. Actually, ethanol rinsing is used at the final stage of SAM preparation to remove any possible SAM on SAM. Regarding this point, we rinsed a SAM substrate after laser ablation in ethanol and observed the middle region by STM. STM images of the same sample before and after rinse are displayed in Figure 5. Immediately, it is it clear that the protrusions survive ethanol rinse. No obvious decrease in size of the protrusions was noticed, though their density might have slightly decreased. From this experimental result, we exclude case 2, thus the protrusions are not SAM islands on SAM. Also the result shows that the protrusions are firmly adsorbed to the SAM substrates, a feature that would be preferred in any practical use.

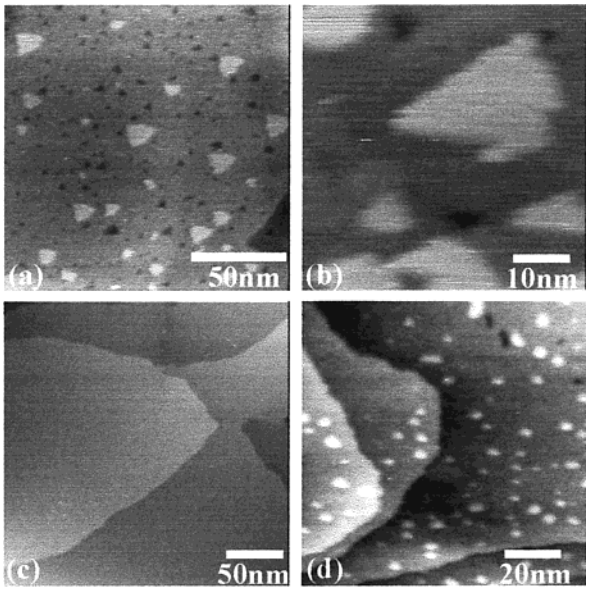

Figure 6. (a) An STM image of SAM islands fabricated by the vapor method. (b) Enlarged STM image. (c) STM image taken 1 day after. (d) STM image of a SAM (hexanethiol) substrate taken two months after exposure to ablation

3.2. Case 3: SAM Islands. Another possibility is that SAM in the middle region is partly damaged and the protrusions are SAM islands on Au. In this scenario, (1) SAM close to the ablation spot is totally blown away, (2) SAM in the middle region is partly blown away, and (3) the remaining SAM islands are observed as protrusions. SAM in the far regions is not damaged. No Si nanoparticles exist on the surface. We exclude this possibility by fabricating real SAM islands and by comparing the characteristics of SAM islands with the protrusions. SAM islands can be easily made by exposing an Au substrate to vapor of hexanethiol. Typical STM images of SAM islands fabricated by the vapor method are shown in Figure 6a and Figure 6b. Even though the size of the SAM islands is on the same order of that of the protrusions, their shapes differ significantly; the protrusions are round shaped while the shape of the SAM islands resembles triangles. Another, and critical difference between the SAM island and protrusion is their stabilities. SAM islands are very unstable and desorb easily leaving a clean Au surface, while the protrusions are very stable. This aspect is demonstrated in Figure 6c, an STM image of a substrate where the SAM islands were observed one day before, and Figure 6d, an STM image of the protrusions taken two months after laser ablation. While the SAM islands dissipate in a day, the protrusions remain even for two months. No obvious decrease in size of the protrusions with time was noticed, though their density gradually decreased. From this experimental result, we exclude case 3, thus the protrusions are not SAM islands on Au. Also the result shows that the protrusions adsorbed to the SAM substrates are stable, a point that would be important in practical use.

3.3. Case 4: Si Nanoparticles on Au. The last possibility is that the SAM is completely blow away and the protrusions are Si nanoparticles deposited on Au. We exclude this possibility by listing up some evidence that shows or indicates existence of SAM on the surface. First, and most directly, in some most high-resolution STM images, the atomic structure of SAM was observed. Second, the density, shape, and size of the etch-pits on the substrate exposed to ablation in the middle region (at where the protrusions are observed) were the same with a clean SAM. In situations where the SAM is supposed not to exist, the density of etch-pits has significantly decreased (Figure 3a,

an image taken close to the ablation spot) or no etch-pits were observed (Figure 6c, an image of a substrate where SAM islands were observed one day before). We thus consider the existence of the etch-pit as an indirect evidence of the presence of SAM. From these experimental result, we exclude case 4, thus the protrusions are not Si nanoparticles on Au.

3.4. Atomic Force Microscopy Observations. The experimental results presented so far are easily explained if we consider the protrusion as Si nanoparticles, though are difficult to explain in other cases. The problem of the STM observations is that the height of the protrusion is measured around 0.4 nm, a value that is substantially smaller than the lateral size. It should be noted that the height of the protrusions did not change on SAMs that have different lengths of alkyl chain (SAM made of pentanethiol, hexanethiol, and octanethiol), a result that gives another evidence that the protrusions are not composed from SAM. As STM measures the electronic structure, the height of a feature in STM does not necessarily correspond to their real topographic height. This is particularly true for organic materials or semiconductor nanoparticles, and the generally tendency is that the height measured by STM is smaller than the real height. To address this problem, we turned to atomic force microscopy (AFM). The lateral feature resolution obtained by AFM is determined in large part by the size and shape of the imaging probe tip, though the measured height of a feature reflects the actual height fairly well. A typical noncontact AFM image (Figure 7a) of the protrusions and their cross section (Figure 7b) shows that the height of the protrusions are around 7 nm, a value substantially larger than the height measured by STM. Taking into considerations these points, we observed the same SAM substrate exposed to laser ablation by STM and AFM, from which the lateral size histogram (Figure 7c) of the protrusions was constructed from the STM images, and the height histogram (Figure 7d) was made from the AFM data. Immediately, it is clear that the mean lateral size and height of the protrusions are very similar, implying that the shape of the protrusions is close to a sphere.[22] The height of the protrusions measured by AFM gives another strong evidence that the protrusions are not composed from SAM. In addition, a photoluminescence measurement of these particles presented in Figure 8 shows an emission peak centered at 623 nm, a value that is in the range of the characteristic emission wavelengths of Si nanoparticles. This result implies that Si nanoparticles exist on the surface. Summarizing all of the experimental results and discussions, we conclude that the protrusions are Si nanoparticles on SAM.

3.5. Control of Size of Si Nanoparticles. We demonstrate that it is possible to control the average size of nanoparticles deposited on SAM. Size of the nanoparticle is the most important factor that determines the degree of the quantum confinement effect, and consequently, the electronic and optical properties of the nanoparticles. Control over the size of Si nanoparticles deposited on Si substrates has been achieved by a simple method of changing the ambient pressure.[13,14] To demonstrate this aspect of nanoparticle engineering, we fabricated Si nanoparticles in different Ar gas ambient pressures and deposited them on SAM. A substantial increase of the size of the nanoparticles fabricated at 10 Torr (Figure 9b) was observed compared to those fabricated at 2 Torr (Figure 9a), showing that it is possible to control the size of the Si nanoparticles deposited on SAM, a point that is of extreme importance to fabricate layers of Si nanoparticles with artificially controlled characteristics.

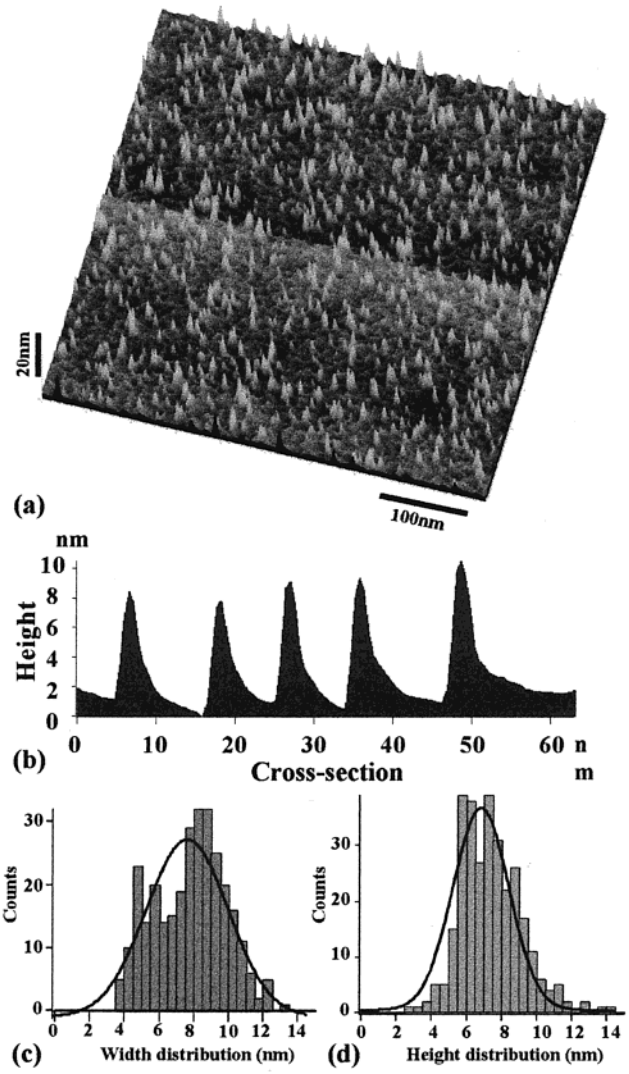

Figure 7. (a) A NC-AFM image of a SAM (hexanethiol) substrate exposed to ablation. (b) Cross section of Si nanoparticles. (c) Histogram of widths of Si nanoparticles measured from STM images. (d) Histogram of heights of Si nanoparticles measured from AFM images. Both histograms were constructed from observations carried out on the same sample.

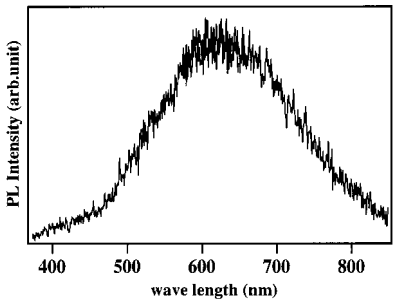

Figure 8. Photoluminescence of the Si nanoparticle deposited on SAM excited at 325 nm.

4. Conclusion

We report that SAM endures fierce conditions during the laser ablation process, and that it is possible to deposit in-situ Si nanoparticles fabricated by laser ablation on SAM. Si nanoparticles deposited on SAM show several promising characteristics that would be appreciated in any future nanodevice applications. They were round shaped, firmly attached to the surface, and remained stable for at least a couple of months.

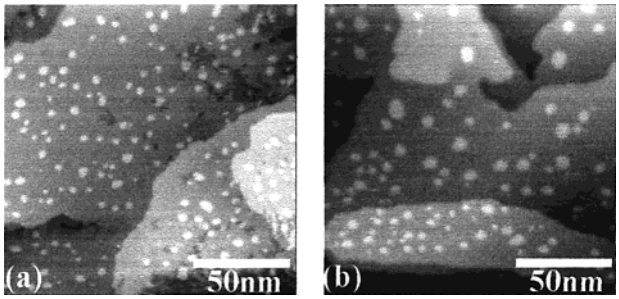

Figure 9. Control over the average size of the Si nanoparticles. STM images of SAM (hexanethiol) substrates exposed to ablation with different ambient pressures. (a) 2 Torr. (b) 10 Torr.

Control over the size of the Si nanoparticles, in the region where quantum confinement effect is important, could be easily achieved by changing the Ar ambient pressure. This encouraging result suggests the possibility of fabricating thin layers of Si nanoparticles that have controlled optical and electronic properties.

In-situ deposition is important since subsequent processes such as vacuum deposition could be carried out sequential to fabricate electronic contacts or protecting capped layers without exposing these easily oxidized materials to air. When oxidized, the oxidized layer would prevent carrier injection to the core of the nanocrystal, impeding fabrication of light emitting devices. The oxidized layer might also determine the physical properties of the nanoparticle, hindering the ability to artificially control the properties of nanoparticle by changing their size.

We believe that the ability of SAM to serve as a template to deposit nanomaterials fabricated by laser ablation should open up a new opportunity to assemble many nanomaterials into new nanoarchitectures. Numerous combination of the available SAMs, fabricated on different substrates and different in chemical and electronic properties, and the wide variety of nanostructures possible to fabricate by laser ablation should provide many interesting aspects to be pursued in the future. Some future suggested applications include control of the chemical functionalities of the SAM surface to achieve selective adsorption of Si nanoparticles through which deposition of nanoparticles on desired locations could be achieved.[23]

Acknowledgment. The support of a Grant-in-Aid for Scientific Research from the Ministry of Education, Science and Culture of Japan is also acknowledged.

References and Notes

(1) Kumar, A.; Whitesides, G. *Appl. Phys. Lett*. **1993**, *63*, 2002.
(2) He, H. X.; Zhang, H.; Li, Q. G.; Zhu, T.; Li, S. F. Y.; Liu, Z. F. *Langmuir* **2000**, *16*, 3846.
(3) Dorogi, M.; Gomez, J.; Osifchin, R.; Andres, R. P.; Reifenberger, R. *Phys. Rev. B* **1995**, *52*, 9071.
(4) Huang, S.; Mau, A. W. H.; Turney, T. W.; White, P. A.; Dai, L. *J. Phys. Chem. B* **2000**, *104*, 2193.
(5) Huang, Z.; Wang, P. C.; Macdiarmid, A. G.; Xia, Y.; Whitesides, G. *Langmuir* **1997**, *13*, 6480.
(6) Owens, R. W.; Smith, D. A. *Langmuir* **2000**, *16*, 562.
(7) Alivisatos, A. P. *Science* **1996**, *271*, 933.
(8) Canham, L. T. *Appl. Phys. Lett*. **1990**, *57*, 1046.
(9) Kanemitsu, Y.; Futagi, T.; Matsumoto, T.; Mimura, H. *Phys. Rev. B* **1994**, *49*, 14732.
(10) Cullis, A. G.; Canham, L. T.; Calcott, P. D. J. *J. Appl. Phys*. **1997**, *82*, 909.
(11) Mason, M. D.; Credo, G. M.; Weston, K. D.; Buratto, S. K. *Phys. Rev. B* **1998**, *80*, 5405.
(12) Werwa, E.; Seraphin, A. A.; Chiu, L. A.; Zhou, C.; Kolenbrander, K. D. *Appl. Phys. Lett*. **1994**, *64*, 1821.
(13) Yoshida, T.; Takeyama, S.; Yamada, Y.; Mutoh, K. *Appl. Phys. Lett*. **1996**, *68*, 1772.
(14) Makimura, T.; Kuni, Y.; Murakami, K. *Jpn. J. Appl. Phys*. **1996**, *35*, L735.
(15) Makimura, T.; Sakuramoto, T.; Murakami, K. *Appl. Phys. Lett*. **2000**, *76*, 1401.
(16) Kroto, H. W.; Hearth, J. R.; Brien, S. C. O.; Curl, R. F.; Smalley, R. E. *Nature* **1985**, *318*, 162.
(17) Iijima, S. *Nature* **1991**, *354*, 56.
(18) Moarles, A. M.; Lieber, C. M. *Science* **1998**, *279*, 208.
(19) Haddon, R. C.; et al. *Nature* **1991**, *350*, 320.
(20) Cui, Y.; Duan, X.; Hu, J.; Lieber, C. M. *J. Phys. Chem. B* **2000**, *104*, 5213.
(21) Poirier, G. E. *Langmuir* **1997**, *13*, 2019.
(22) It is unclear why the STM tip does not seriously perturb (and sweep away) the Si nanoparticles.
(23) Hata, K.; Fujita, M.; Yoshida, S.; Yasuda, S.; Makimura, T.; Murakami, K.; Shigekawa, H.; Mizutani, W.; Tokumoto, H. *Appl. Phys. Lett.* **2001**, *79*, 692.